J. Earth Syst. Sci. (2022)131 163
https://doi.org/10.1007/s12040-022-01909-x

Insights into petrogenetic processes from a part of the Eastern Deccan Volcanic Province, India, using cluster analyses of mineralo-chemical data

Payel Dey[1], Jyotisankar Ray[1,*], Janisar M Sheikh[2], Suresh C Patel[2], Christian Koeberl[3] and Avipsha Chakraborty[1]

[1]*Department of Geology, University of Calcutta, 35, B.C. Road, Kolkata 700 019, India.*
[2]*Department of Earth Sciences, Indian Institute of Technology Bombay, Powai, Mumbai 400 076, India.*
[3]*Department of Lithospheric Research, University of Vienna, Althanstrasse 14, 1090 Vienna, Austria.*
**Corresponding author. e-mail: jsray65@hotmail.com*

MS received 21 September 2021; revised 13 February 2022; accepted 23 February 2022

Multivariate statistical analysis involving hierarchical clusters was carried out for basaltic samples (and associated units) from Khandwa (21°49′N, 76°21′E). 'Highly significant' or 'significant' linear correlation coefficient values (r) corresponding to different minerals (namely, olivine, clinopyroxene and plagioclase), denote several oxides (as for example, MgO, FeO, SiO_2, Al_2O_3, Na_2O, CaO and TiO_2) which were used for construction of dendrograms. Critical analysis of hierarchical patterns revealed that at the outset of magmatic crystallization, heterogeneous (∼greater symmetry) clusters are present. For the crystallization of the lava flows, the 'bulk level of crystallization' (in respect of clinopyroxene and plagioclase) varies from ∼30 to ∼60%, whereas their 'ultimate crystallization' appears to be quite high (∼80 to ∼97%). The bulk crystallization of the lava flows shows a broad control of ambient temperature. The dyke system (feeder dyke and chilled dyke) also shows bulk crystallization pattern similar to that of lava flows. Cluster analyses for basement gabbroic rock suggest that there is a wide compositional spectrum for the cumulate portion, whereas the intercumulus portion is marked by relatively restricted compositions. In general, the present CA (cluster analysis) clearly indicates progressive amalgamation of clusters (and their concomitant fall of symmetry) with advancing differentiation.

Keywords. Eastern Deccan Volcanic Province; cluster analysis; dendrogram patterns; feeder dykes; bulk level of crystallization; ambient temperature.

1. Introduction

Mineral chemistry data of flood basalt provinces often play an important role as significant petrogenetic assessor (Marzoli *et al.* 1999; Dey *et al.* 2021). Although for flood basalt provinces, high precision major, trace and isotopic data are regarded as sensitive petrogenetic indicators, mineral chemistry data serves as significant tool (in association with whole-rock geochemical data) for

This article is part of the Topical Collection: Deccan Traps and other Flood Basalt Provinces – Recent Research Trends.

Supplementary material pertaining to this article is available on the *Journal of Earth System Science* website (http://www.ias.ac.in/Journals/Journal_of_Earth_System_Science).

Published online: 23 July 2022

finger printing petrogenetic processes (Moraes *et al.* 2018; Macedo Filho *et al.* 2019). In some cases, the mineral chemistry data alone have been rewardingly used to unravel certain primary magmatic features like appearance of liquidus temperatures of different minerals, oxygen fugacity and magma density (Ganguly *et al.* 2012; Rao *et al.* 2012). In the case of Deccan flood basalt province, importance of using such mineral chemical data has recently been highlighted by Dey *et al.* (2021). The mineral chemistry data interpretation can be extended to almost all flood basalt provinces. For recognition of magma chamber processes, the importance of mineral chemistry data has been dealt with in detail for Deccan Volcanic Province (Melluso and Sethna 2011; Ganguly *et al.* 2012; Rao *et al.* 2012). Considering the significance of mineral chemistry data (for understanding the petrogenetic processes of flood basalt provinces) in the backdrop, the approach of cluster analysis (involving mineralo-chemical data) for several volcanic rocks was taken up by Tibaldi (1995), Mazzarini (2004), Mazzarini *et al.* (2010). In fact, cluster analysis refers to a simple process of grouping a set of objects in such a way so that the objects in the same group known as cluster, are more similar in some sense to each other than those in other groups (clusters) (Le Maitre 1982). A good resultant of cluster analysis will give rise to a number of clusters where within each such cluster some observations remain as similar as possible. Cluster analysis does not differentiate between dependent and independent variables and after cluster analysis, the number of observations or cases becomes consolidated (or amalgamated) into smaller set of clusters. The basic flow of cluster analysis involves decisive algorithm where all the data are initially considered as a single group, and subsequently, it is subdivided according to some specified parameter (or criterion) until each group contain only one object. This method of clustering involves construction of several dendrograms and may be successfully employed to understand magma source (Valentine and Perry 2007; Germa *et al.* 2013; Tadini *et al.* 2014; Cortes *et al.* 2015). In a multiphased lava system and associated dykes, cluster analysis may reveal useful information on feeder dyke orientation (Tibaldi 1995; Korme *et al.* 1997; Corazzato and Tibaldi 2006; Paulsen and Wilson 2010; Bonali *et al.* 2011). In Deccan basalts, use of statistical analyses has been gainfully used to build up a cogent petrogenetic model in recent years by Shrivastava *et al.* (2014).

In the present contribution, an attempt has been made to employ cluster analysis of a huge number of available mineral chemistry data (Dey *et al.* 2021) of parts of Eastern Deccan Volcanic Province (EDVP) near Khandwa (21°49′N, 76°21′E), Madhya Pradesh, India. The outcome of such cluster analysis will be interesting in the sense that it will help to understand the inherent magmatic processes of specific parts of Deccan Volcanic Provinces (DVP) (having silica saturated/oversaturated characters) based on multivariate analysis or 'grouping' method. Moreover, the outcome of cluster analysis for basaltic rocks of Khandwa will address almost all of its petrogenetic tenets except the remaining portion that involves elucidation of whole rock geochemical model.

2. Regional geology

The Deccan Volcanic Province (DVP) has profound importance in the global context because of its large spatial distribution, huge volume and specific eruption-duration, which broadly corresponds to K–T boundary (Duncan and Pyle 1988; Baksi 1994; Hull *et al.* 2020). Mantle melting processes, development of lava flows and plumbing systems of dyke-sills offer great scope for understanding petrogenetic processes in continental flood basalt provinces (Coffin and Eldholm 1994; Self *et al.* 1997; Eldholm and Coffin 2000; Ernst and Buchan 2001; Rajan *et al.* 2005; Sheth *et al.* 2009).

Within the vast expanse of DVP, the quantum of studies vary from one sector to another. For example, the southwestern and western parts are geologically well studied (Mahoney *et al.* 1982; Lightfoot and Hawkesworth 1988; Peng *et al.* 1994; Bondre *et al.* 2006) and the development of lavas in the western and southwestern sector has been relegated to Satpura Narmada Tapi rift system as suitable channel ways (Crookshank 1936; West 1958; Baksi 1994; Sen and Cohen 1994; Bhattacharjee *et al.* 1996; Kumar and Shrivastava 2009; Kashyap *et al.* 2010; Shrivastava *et al.* 2014, 2017; Pathak *et al.* 2017). The Eastern Deccan Volcanic Province (where the present study area belongs to) is a relatively lesser attended section where geological studies have been carried out in sporadic sectors at different point of time (Crookshank 1936; Alexander and Paul 1977; Deshmukh *et al.* 1996; De 1996; Nair *et al.* 1996; Yedekar *et al.* 1996; Peng *et al.* 1998; Pattanayak and Shrivastava 1999; Ahamad and Kumar 2008). However, during the

last 20 years, for EDVP, a plethora of information involving petrogenetic aspects, mineral chemistry, existence of liquid immiscibility and lava morphology has been generated (Mahoney *et al.* 2000; Sengupta and Ray 2007; Duraiswami *et al.* 2008; Kashyap *et al.* 2010; Sengupta and Ray 2011a, b; Ganguly *et al.* 2014; Srinivas *et al.* 2019; Dey *et al.* 2020, 2021; Kale *et al.* 2020). However, a well-demarcated 'chemostratigraphy' (as existing in Western Deccan Volcanic Province; Cox and Hawkesworth 1985; Beane *et al.* 1986) in EVDP is yet lacking. Shrivastava *et al.* (2015) presented ^{40}Ar–^{39}Ar age data from basaltic lavas of the Mandla lobe (64.21 ± 0.33 Ma) occurring at the eastern margin of Deccan Volcanic Province. According to Shrivastava *et al.* (2015), the lavas of Mandla lobe appears to be younger than the main Deccan volcanic activity of the Western Ghats (∼67–65 Ma).

3. Present study

The present investigation was carried out around Khandwa (21°49′N, 76°21′E), which forms a part of Eastern Deccan Volcanic Province, lying at the Nimur district, Madhya Pradesh, India (figure 1a). For the preparation of geological map of the area (figure 1b), three-tier classification of De (1974) was used. The physical volcanological characters of this study area were earlier given by Dey *et al.* (2020, 2021).

3.1 *Mode of occurrence*

The study area reveals characteristic development of three flows (flow I, flow II and flow III) with different degrees of prominence and development of chilled facies for flow I and flow II. Coarse-grained gabbroic cumulate rock (apparent basement to the lava flows) has also been noted. Characteristic presence of feeder dyke (FD) and chilled dyke (CD) was also recorded in this area. The feeder dyke is found to be associated with flow II and maintains a strike direction of 75°–78° being located at 327 m height. The chilled dyke, on the other hand, is also associated with flow II and runs with almost east-west strike at an elevation of 309 m. In the field, the chilled dyke gives a cross-cutting relation with flow II. The sample locations (corresponding to several structural zones belonging to different flows) have been shown in figure 1(b) for easy understanding for the readers. Moreover, presence of two small but prominent marker horizons is found. These are intertrappean beds between flow I and flow II and between flow II and flow III (figure 1b). A geological map has been prepared based on the identification of several characteristic zones within each lava flow, which are Lower Vesicular Zone (LVZ) grading upward to Lower Colonnade Zone (LCZ), the Entablature Zone (EZ) and the Upper Colonnade Zone (UCZ) grading upward to Upper Vesicular Zone (UVZ) (De 1974) (figure 1b). In majority of the places, different zones within the lava flows show good exposure, but in some cases, their presence can be studied in subcrop as well. The lava flows are by and large fresh and unaltered but in some cases, they show development of spheroidal weathering and highly altered vesicular zone. Representative photographs highlighting prominent field features have been given in figure 2(a–f).

3.2 *Petrography*

For all three lava flows, clinopyroxene, plagioclase (and rarely olivine) are the main phenocrystal phases. The groundmasses are represented by smaller-sized clinopyroxene, tiny plagioclase, opaque mineral, microlites and glass (often devitrified). The proportions of individual minerals are not constant; on the contrary, their presence is zone-specific (for example, glass is more dominant in vesicular zones). Ophitic, subophitic, porphyritic, glomeroporphyritic, intersertal and vitrophyric textures are commonly displayed in these lava flows. For both feeder and chilled dykes, plagioclase and clinopyroxene occur both as phenocryst and groundmass. Textures for dyke rocks are similar to that of the lava flows. The apparent basement rock (coarse-grained gabbro) consists of relatively coarse grains of subhedral plagioclase, prismatic clinopyroxene and some opaque minerals, which correspond to cumulus minerals. The intercumulus (relatively fine-grained) minerals are represented by smaller plagioclase and clinopyroxene. Overall this gabbroic basement represents cumulus and intercumulus textural patterns. Representative photomicrographs of different units in the study area have been shown in figure 3(a–f).

3.3 *Mineral chemistry*

Electron microprobe analysis (EPMA) of constituent mineral phases of the three lava flows,

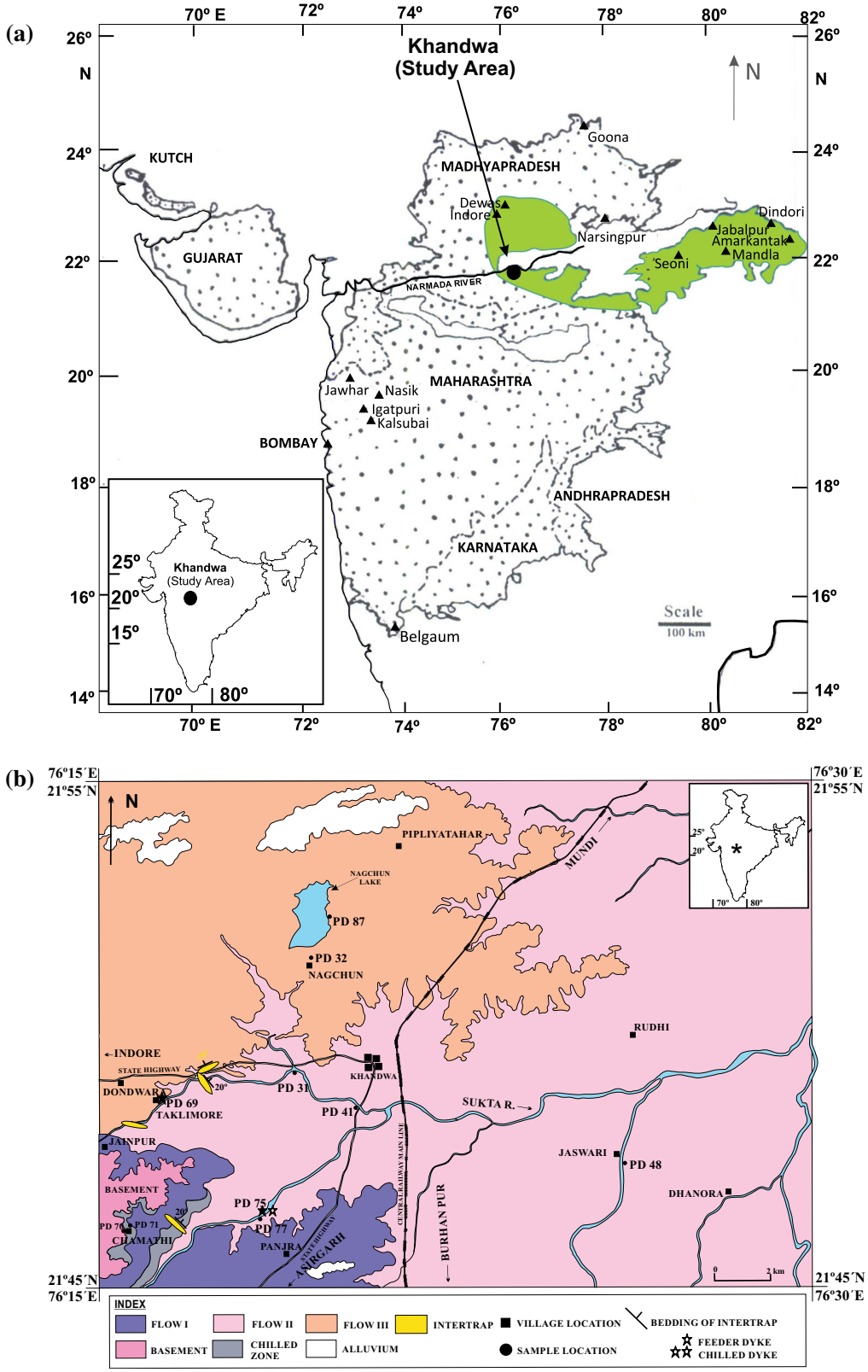

Figure 1. **(a)** Overall distribution of Deccan Volcanic Province (stippled) in India. Green areas mark the extent of Eastern Deccan Volcanic Province (EVDP) after Kashyap *et al.* (2010). Solid circle indicates present study area. **(b)** Geological map of the present study area (prepared by present authors). Locations of study samples (e.g., PD 48, PD 41, etc.) have been shown in this map. Star in the inset map denotes the study area.

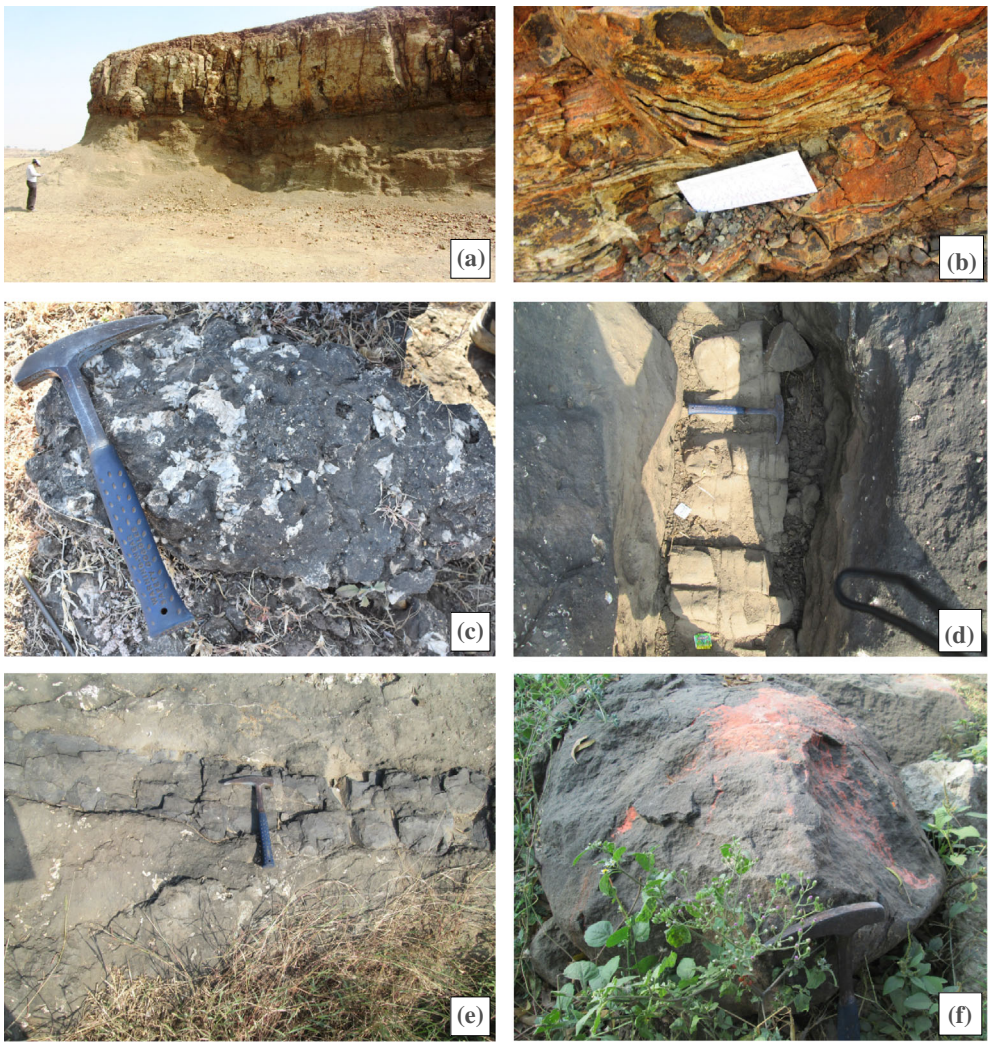

Figure 2. Field photographs showing **(a)** Development of UCZ and EZ in flow III near Nagchun. **(b)** Prominent EZ in flow III near Nagchun Village. **(c)** Upper vesicular zone filled in with abundantly developed zeolite amygdules in flow II. **(d)** Prominent Feeder dyke associated with flow II. **(e)** Laterally extensive chilled dyke found to be closely associated with flow II near Panjra area. **(f)** Coarse-grained gabbroic apparent basement in Chamathi village.

dyke rocks and apparent cumulate gabbro basement were performed at the Department of Earth Sciences, IIT Bombay, India, using CAMECA SX-Five Electron Probe MicroAnalyser (EPMA). The analytical conditions for the instrument were: acceleration voltage of 15 kV, beam current of 20 nA and beam diameter of 1 μm. Both natural and synthetic standards were used for calibration of the elements and data correction was done by X-PHI method.

It needs to be mentioned that different constituent minerals, namely, olivine, clinopyroxene, and plagioclase are not developed in different flows (or zones) in equal prominence. The flow/zone/dyke/or cumulate rock-wise distributions of different minerals of the investigated area are given in table 1. EPMA of olivine, clinopyroxene and plagioclase (phenocrystal data) has been furnished in Supplementary tables S1–S3, respectively.

4. Selection and significance of suitable major elements

Correlation coefficients of several major oxides are often determined to understand their nature of significance to elucidate petrogenetic history of a given unit of rock (Saha *et al.* 1974; Hazra *et al.* 2010). The routine task is to find out the significance levels of obtained correlation coefficient values in respect of several major oxides bivariate diagrams for mineral phases. 'Highly significant' or 'significant' major oxides are next shortlisted (and

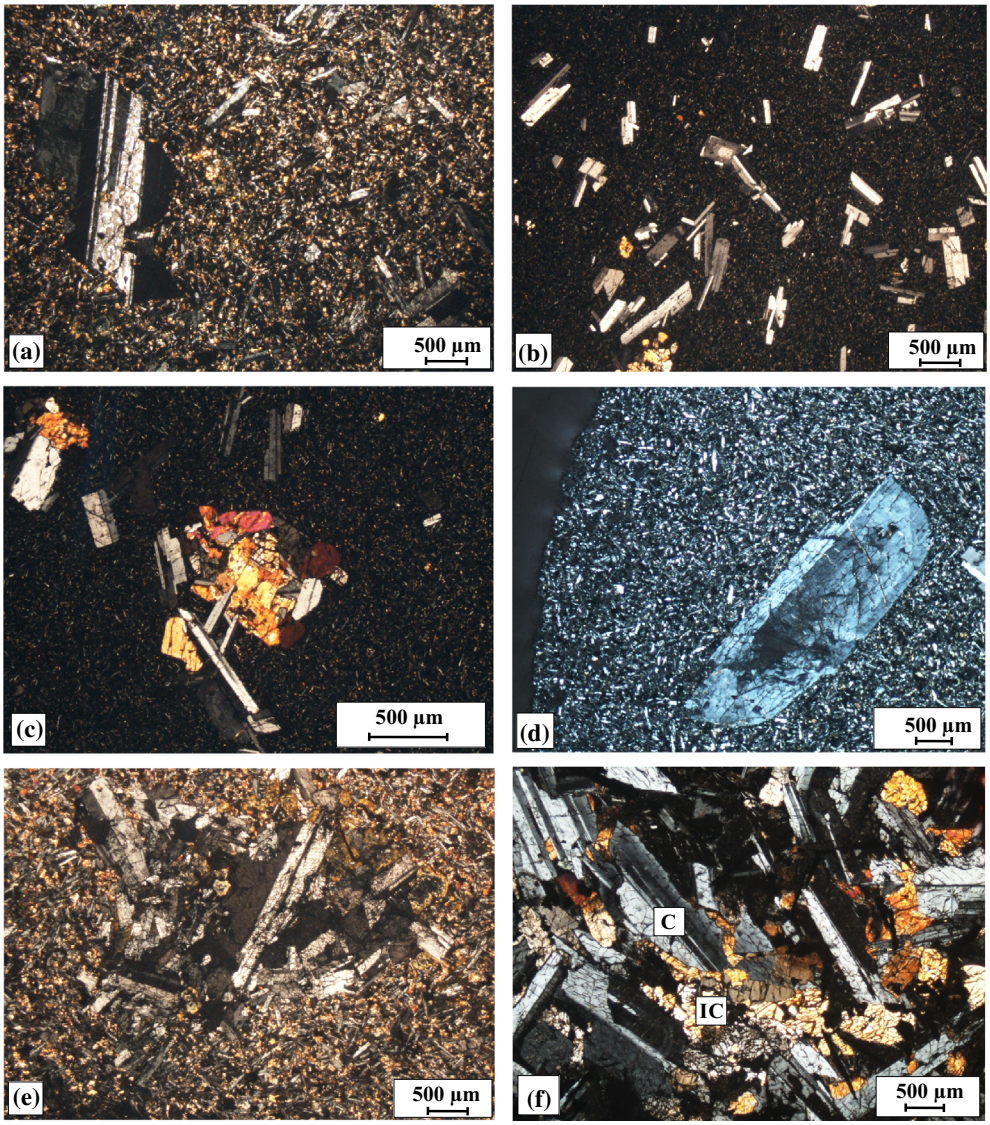

Figure 3. Photomicrographs showing **(a)** Large zoned phenocryst of plagioclase (set in a finer groundmass) in feeder dyke. Relatively fine-grained plagioclase grains are also noticed in the groundmass. **(b)** Dispersed elongated plagioclase phenocrysts in chilled groundmass material (flow I chilled zone). Few clinopyroxene (micro) phenocrysts are noticed. **(c)** Phenocrysts of relatively coarse clinopyroxene and plagioclase showing subophitic relation. These phenocrysts are set in chilled groundmass (flow I chilled zone). **(d)** Large strongly zoned plagioclase phenocrysts embedded in cryptocrystalline and glassy groundmass (flow I chilled zone). **(e)** Number of plagioclase phenocrysts are clustered together (and set in a finer groundmass) to give rise to glomeroporphyritic texture (flow II chilled zone). **(f)** Cumulus and intercumulus textural pattern developed in coarse-grained gabbroic rock (apparent basement). The cumulus (C) portion is mostly marked by coarse plagioclase, while intercumulus (IC) portion is represented by smaller clinopyroxene and plagioclase.

used) in the present study because such highly significant/significant correlation values are considered to be helpful to elucidate petrogenetic history (Saha *et al.* 1974). Supplementary table S4 gives such shortlisted 'highly significant' (or 'significant'/occasionally non-significant) correlation coefficient for different minerals. Based on these significance levels of '*r*' (Snedecor and Cochran 1967), for olivine, two important oxides MgO and FeO have been selected. For plagioclase, four variables, namely, SiO_2, Al_2O_3, Na_2O and CaO were chosen. Following six variables namely, SiO_2, TiO_2, Al_2O_3, FeO, MgO and CaO for clinopyroxene were found to be important.

4.1 *Multivariate statistical analysis and dendrogram construction*

In our present study, major element mineral chemical data were subjected to multivariate statistical analysis, which involve hierarchical division, cluster analysis and construction of

Table 1. *Flow/zone-wise occurrences of different constituent phenocrystal minerals in the study area.*

Name of the mineral	Lava/zonewise occurrences type	EPMA data presented in	Comments
Olivine	Flow II UCZ	Supplementary table S1	Olivine occurs as very tiny, discrete phenocrysts in flow II. Fo ranges from ∼41 to ∼52, possibly suggesting evolved nature of olivine caused due to magmatic reaction
Clinopyroxene	All the units incorporating flow I, flow II, flow III, FD, CD and apparent basement	Supplementary table S2	There is a huge compositional spectrum considering all the three lava flows and other units corresponding to the respective degree of differentiation
Plagioclase	All the units incorporating flow I, flow II, flow III, FD, CD and apparent basement	Supplementary table S3	The sizable variations of anorthite content considering all the three lava flows and other units correspond to different degrees of magmatic differentiation (possibly aided by changing PH_2O conditions)

Note: Other phases of the investigated rocks include groundmass glass and opaque minerals (ilmenite and magnetite). These are not included in the cluster analysis study. For explanation of abbreviations, see text.

dendrogram using PAST software. Details of PAST software used in the present study is given in Supplementary materials.

5. Dendrograms and mineral-wise pattern identification

In the present study, hierarchal clustering method with agglomerative algorithm was employed for major oxides of clinopyroxene, plagioclase and olivine. Standardized Euclidean distances between samples were computed following Le Matrie (1982). In all cases, the horizontal (base level) axis denotes the point numbers of analyses of different relevant minerals (see Supplementary tables S1–S3), while the vertical axis refers to Euclidian distance. This distance, in fact, represents progressive magmatic differentiation and consequent fall of symmetry patterns with respect to the initial ones.

5.1 *Olivine*

Olivine phenocryst is recorded only from flow II and that too in small amount. The dendrogram pattern of olivine shows 10 initial data points with gradual amalgamation giving rise to smaller number of clusters. At a moved distance of 3 (out of 9), the initial 10 clusters reduced down to two, and this corresponds to about 33% fractional crystallization of parent magma. In fact, interrelation between magmatic differentiation and clusters (distance) was depicted earlier by Owen (1989). At a moved distance of 8.5 (out of 9), the number of clusters reduces to two and this corresponds to 94% fractional crystallization. The extreme right-hand side (RHS) dendrogram pattern (figure 4) shows no change in the clustering pattern from the beginning to the end of crystallization. This undisturbed pattern (22/1) possibly represents xenocryst of highly differentiated olivine grain inherited from any precursor rock.

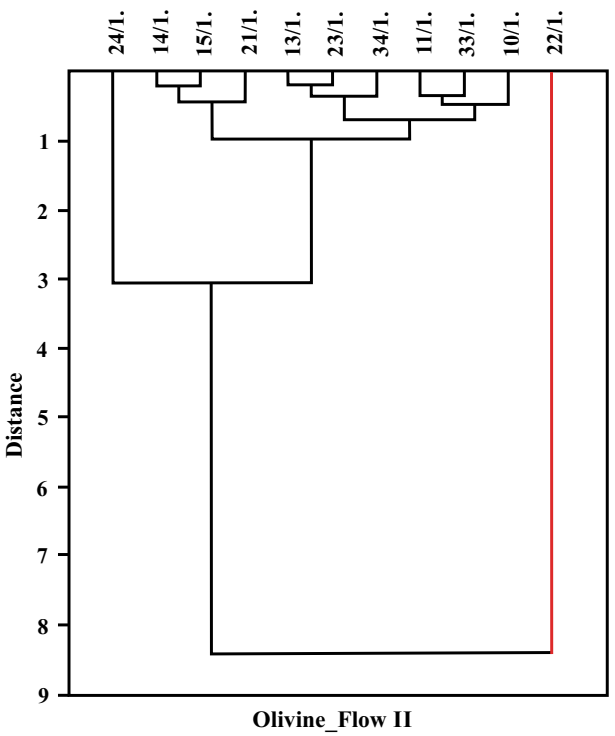

Figure 4. Dendrogram pattern of olivine found in flow II. The bulk level of crystallization is ∼33%. The vertical axis represents Euclidian distance (∼ degree of differentiation). Numerals in the horizontal axis indicate data points of olivine analyses (Supplementary table S1).

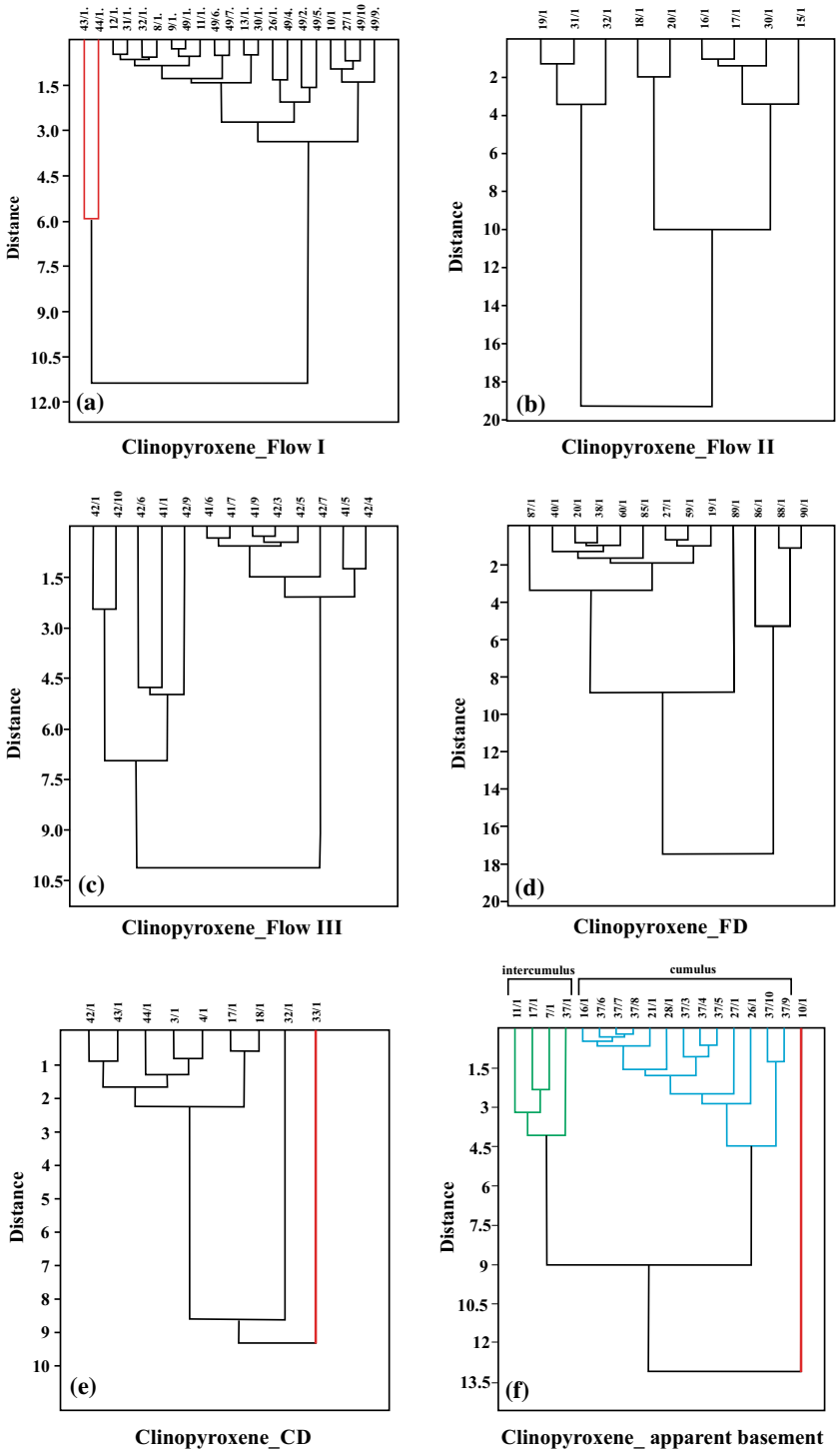

Figure 5. **(a–f)** Dendrogram patterns for clinopyroxene corresponding to different flows/feeder dyke/chilled dyke and gabbroic apparent basement. In each case, vertical axis refers to Euclidian distance (∼ degree of differentiation). Numerals in the horizontal axis indicate data points of clinopyroxene analyses (Supplementary table S2).

5.2 *Clinopyroxene*

Clinopyroxene phenocrystal data are available for flow I, flow II, flow III, feeder dyke, chilled dyke and the (apparent) gabbroic basement rock. For the clinopyroxene of flow I, in general, there are numerous clustering (figure 5a) at the initiation of magmatic crystallization. From the huge number of initial clusters, the pattern reduces drastically at a moved distance of 3.5 (out of 12) which corresponds to 29% fractional crystallization. The differentiation was totally completed at ∼92% (at a

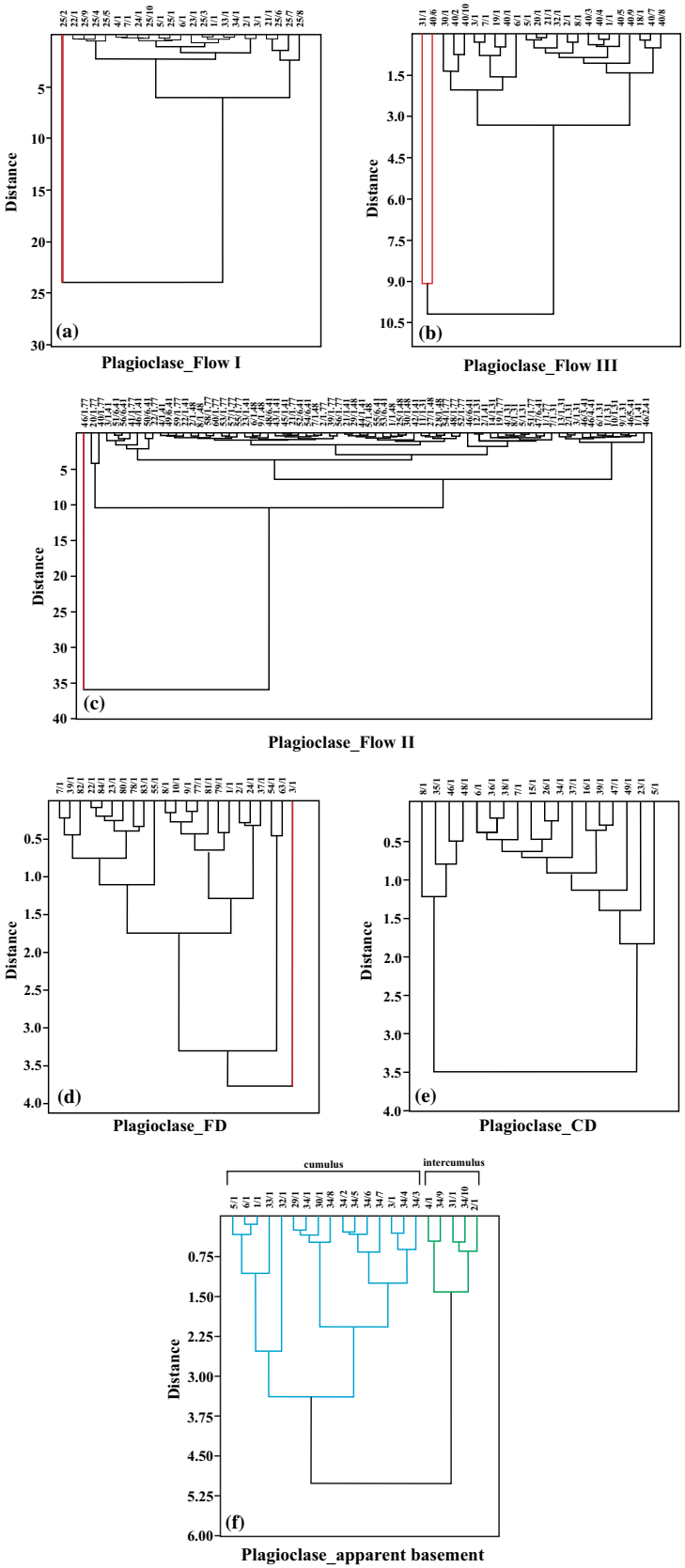

Figure 6. **(a–f)** Dendrogram patterns for plagioclase corresponding to different flows/feeder dyke/chilled dyke and gabbroic apparent basement. In each case, vertical axis refers to Euclidian distance (∼ degree of differentiation). Numerals in the horizontal axis indicate data points of plagioclase analyses (Supplementary table S3).

Table 2. *Degree of bulk level and ultimate crystallization (in %) as revealed from dendrogram analyses.*

	Olivine		Clinopyroxene		Plagioclase	
Units	Bulk level of crystallization (%)	Ultimate crystallization (%)	Bulk level of crystallization (%)	Ultimate crystallization (%)	Bulk level of crystallization (%)	Ultimate crystallization (%)
FI			29	92	20	80
FII	33	94	50	95	25	90
FIII			70	95	38	97
FD			45	–	44	–
CD			25	–	38	–

Note: FI, FII and FIII represent flow I, flow II and flow III, respectively. FD: feeder dyke, CD: chilled dyke.

moved distance of 11 out of 12). The two clusters lying at the extreme left have high FeO content and for the major part of the fractional crystallization, they remained undisturbed. This corresponds to the presence of local ferrohypersthene crystal.

Clusters of clinopyroxene for flow II (figure 5b) on the other hand, show an almost equally evolved pattern and it appears that the major portion of the crystallization was completed at ∼50% (10 moved distance out of 20). The differentiation was finalized at almost ∼95% (19/20×100).

Patterns of the clinopyroxene from flow III show numerous initial clusters (figure 5c). But depending upon their later amalgamation, the cluster pattern can be subdivided into right-hand side (RHS) cluster and left-hand side (LHS) cluster. For the RHS cluster, the bulk of differentiation was complete at a moved distance of 2 (out of 10.5), which corresponds to nearly 20% of fractional crystallization. For the LHS clusters, the ultimate evolution continued up to a more advanced stage of differentiation at a moved distance of 7.3 (out of 10.5) which suggests about 70% fractional crystallization. At the end, the differentiation reached almost 95% (9.5 moved distance out of 10.5), which represents the (extreme) final stage of crystallization.

The cluster pattern for feeder dyke (figure 5d) starts with similar geometry; however, most of the differentiation was completed at ∼45% (moved distance 9 out of 20). The differentiation progressed and finally ceased at ∼89% (moved distance 17.8 within 20).

For the cluster pattern of chilled dyke (figure 5e), only one data point from the beginning was highly differentiated (extremely RHS data point), whereas the other data points showed equal level of heterogeneity (LHS cluster pattern). For this data point (LHS), differentiation in bulk level was almost complete at 25% (2.5 moved distance out of 10). The end part of differentiation is marked at 92% (9.2 moved distance out of 10).

Clinopyroxene from the apparent basement characteristically shows three cluster patterns (figure 5f). The middle dataset suggests cluster pattern that corresponds to effective cumulate portion having relatively higher MgO. The LHS clusters show an apparent grouping having relatively higher FeO, which has been caused due to differentiation of the parent magma from the beginning. It corresponds to crystallization from the left-over (residual) evolved intercumulus liquid. The extreme RHS data points suggest its most primitive nature having the highest MgO and relatively higher FeO, possibly signifying olivine relict. This might have reacted later with the ambient liquid and finally disappeared from the magmatic scenario.

5.3 *Plagioclase*

Plagioclase of flow I (Chilled Zone) shows two broad clusters; which may be divided into extreme RHS cluster and middle cluster (figure 6a). For these two clusters, plagioclase composition becomes broadly identical at about 20% fractional crystallization (6 moved distance out of 30). Finally, plagioclase data points corresponding to these two clusters converge where crystallization ended at almost 80% fractional crystallization (moved distance 24.5 out of 30). One data point in the plagioclase dataset of flow I shows no evidence of clustering and remains undisturbed from the beginning. This possibly suggests an accidental

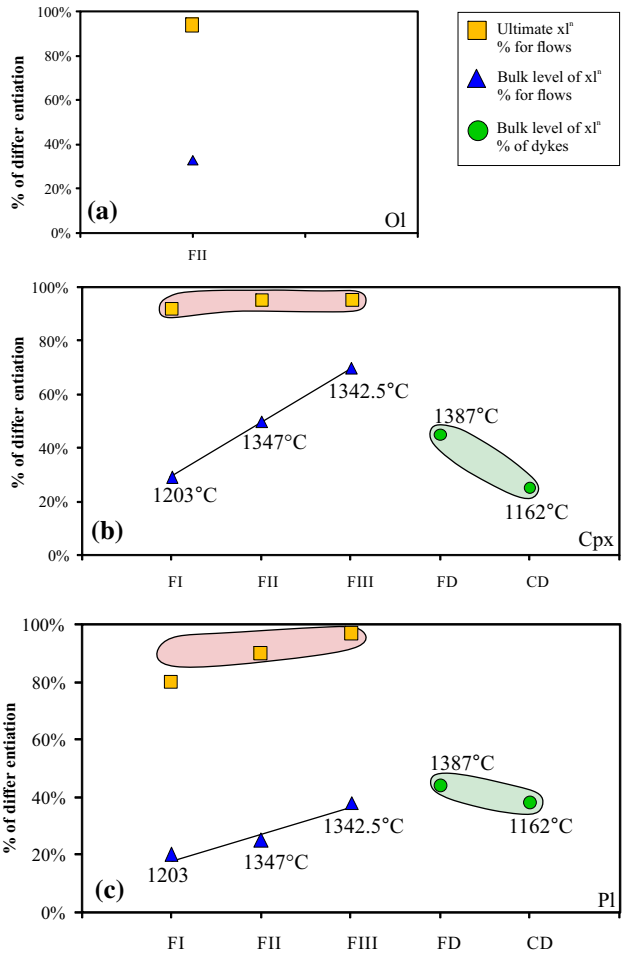

Figure 7. Plot of bulk level of crystallization and ultimate crystallization for **(a)** olivine (Ol), **(b)** clinopyroxene (Cpx) and **(c)** plagioclase (Pl). For both figure 7(b and c), percentage of bulk level of crystallization increases from flow I to III. In case of flow I, flow II and flow III, the deduced thermometry (Putirka 2008) has been denoted. Pattern of crystallization for feeder dyke and chilled dyke has been marked with a different field. Again for figure 7(b and c), it may be noted that fields of maximum extent of crystallization (ultimate crystallization) for lava flows have been shown by separate fields. The ultimate extent of crystallization represents theoretical possibility up to which crystallization may continue. In reality, in all probability, crystallization reached its acme only at its bulk level of crystallization. For both feeder dyke and chilled dyke, only bulk levels of crystallization were the appropriate cases and shown accordingly. For figure 7(b and c), the pink (almost horizontal) elongated field represents ultimate crystallization for lavas, whereas straight line indicates their bulk level of crystallization; the green lensoidal field denotes bulk crystallization of dyke (feeder dyke and chilled dyke). The deduced thermometric values have been incorporated from Dey *et al.* (2021). For figure 7(a–c), FI, FII and FIII represents lava flow I, lava flow II and lava flow III, respectively; FD: feeder dyke, CD: chilled dyke (for details see text).

potash feldspar inclusion within plagioclase where the inclusion is marked by lower CaO (wt.%), lower Na_2O (wt.%) and relatively higher K_2O (wt.%).

In the case of flow III (figure 6b), two data points form a single cluster (extreme LHS) having very low CaO and low Na_2O contents (CaO: 8.2 wt.%, Na_2O: 6.9 wt.% and CaO: 6.8 wt.%, Na_2O: 6.1 wt.%, respectively). This suggests presence of local andesine fragments within highly calcic plagioclase. Besides this, there are two clusters present in this diagram (figure 6a) which may be termed as the middle cluster and the RHS cluster. For both of these clusters, plagioclase composition attained unique (identical) chemistry. The bulk of the differentiation is complete when ∼38% crystallization took place (4 moved distance out of 10.5). The differentiation finally ended at 97% crystallization (10.2 moved distance out of 10.5).

The dataset corresponding to flow II (figure 6c) shows strong initial heterogeneity giving rise to numerous initial clusters. However, despite having initial heterogeneity, the differentiation was completed at ∼25% (10 moved distance out of 40). Final (extreme) point of differentiation was achieved at 90% fractional crystallization (36 moved distance out of 40). It is to be noted that one data point (46/1.77) remains undisturbed from the beginning to the end of crystallization. Highest K_2O of the data point possibly represents a potash feldspar inclusion.

The plagioclase dataset corresponding to feeder dyke is shown in figure 6(d). One data point shows alien character (extreme RHS) and it does not show any trend of differentiation. In all probability, this data point represents xenocrystic plagioclase inherited from a more primitive source. The remaining two clusters (figure 6d), namely the middle cluster and the LHS cluster, show effect of plagioclase differentiation. The differentiation has been significantly advanced at ∼44% (1.75 moved distance out of 4). Finally, the plagioclase crystallization reached its acme at 80% (3.2 moved distance out of 4). Another (almost undifferentiated) cluster (close to data point 3/1) corresponds to extremely differentiated plagioclase having the highest Na_2O and lowest CaO contents.

Plagioclase datasets from chilled dyke form two clusters (LHS cluster and RHS cluster) (figure 6e). The plagioclase composition attained its maximum differentiation at ∼87%, corresponding to both the clusters (3.5 moved distance out of 4). The bulk level of crystallization was, however, noted to be 38% (1.52 moved distance out of 4).

Plagioclase datasets for the apparent gabbroic basement (figure 6f) have two parts: the RHS cluster represents intercumulus portion and

denotes relatively restricted range of composition. On the other hand, the LHS cluster shows a variable composition. For this, the most evolved plagioclase composition attained ∼60% fractional crystallization of the parent magma (3.70 moved distance out of 6).

6. Discussion

It is apparent that multivariate statistical analysis (and construction of dendrograms and mineral-wise pattern identification) involving mineral chemical data for the present study indicates mineral-specific cluster patterns. The primitive (early formed) olivine is quite restricted in occurrence and has been detected only in flow II with a less modal proportion. It may happen that olivine-impoverishment may be related to subsequent destruction or decadence of early formed olivine by reaction with the ambient magma (Jennings *et al.* 2019). For all the three phenocrystal phases (namely, olivine, clinopyroxene and plagioclase), in some of the lava units or dyke system, there are some alien data points in the dendrogram patterns. These alien data points do not show any further segmentation during the crystallization process and can be interpreted as representing some xenocrystic mineral composition or some stray inclusion. Apart from this alienation, the other majority of the datasets show progressive amalgamation of dendrogram clusters and decrease in symmetry patterns. For the convenience of understanding, the degree of bulk crystallization pattern as well as terminal stage of crystallization for olivine, clinopyroxene and plagioclase have been given in table 2 and figure 7(a–c). Corresponding thermometric values have also been shown in figure 7(a–c) to decipher the interrelation between degree of crystallization and thermal ambience. Figure 7(a) shows that the modally deficient olivine could complete its bulk crystallization at almost ∼33% fractional crystallization; although there is an indication from dendrogram pattern (figure 4) that the olivine crystallization might have continued up to 90% differentiation. This may be discounted considering modal decadence of olivine in the present case. Figure 7(b) shows that for the bulk of the crystallization pattern (for clinopyroxene), there is a positive correlation between the relative degrees of crystallization and deduced thermometric values. For terminal crystallization behaviour of clinopyroxene, however, there is not much change and it is varying from ∼90 to ∼95%. The patterns of clinopyroxene crystallization for the feeder dyke (FD) and chilled dyke (CD) are distinctly different. For the FD, the crystallization continued up to ∼50%, whereas for the CD, the crystallization pattern could proceed up to ∼30%, where the chance of advanced crystallization was too low for quick chilling.

Plagioclase crystallization (table 2 and figure 7c) also shows a similar pattern as that of clinopyroxene. In figure 7(c), the terminal stage of crystallization for plagioclase shows a spectrum of ∼80 to ∼97% crystallization. The pattern for plagioclase crystallization in feeder dyke and chilled dyke is drastically different from that of the lava flows. Both the dykes show moderate to low degree of crystallization (∼35 to ∼40%) because of their early chilling behaviour. However, for the feeder dyke, it appears to be active and capable of supplying magma even at a later period of magmatic history.

Apparent basement in the present study is represented by coarse gabbroic rocks. Textural studies further show that these rocks have two distinct parts: (i) the cumulate part corresponding to crystal settling and (ii) intercumulus part that corresponds to the derived or residual liquid. For clinopyroxene datasets, the intercumulus dendrogram pattern is relatively homogeneous, which suggests more restricted composition in the derived liquid. The clinopyroxene cumulus dataset show a relatively greater inhomogeneity which indicates a slight diversity among the settled cumulus clinopyroxene compositions. From the plagioclase datasets, similar restricted nature of intercumulus crystals has been suggested. Plagioclase cumulus crystals also show relative compositional diversity similar to that noted from clinopyroxene dendrogram pattern. The compositional difference between the intercumulus liquid and cumulus crystals can be ascribed to rising magma and sudden transfer below solidus.

This study based on multivariate analysis, therefore effectively helps to identify the cluster patterns for different rock-forming minerals within a portion of Eastern Deccan Volcanic Province. The distinct nature of hierarchical cluster patterns involving different minerals, for several units of the study area can be well discriminated in terms of their bulk and terminal crystallization history.

7. Conclusion

Based on the above study, the following conclusions can be drawn.

- For available mineral chemistry data, some highly significant major oxide variations could be categorically identified.
- Dendrogram pattern analyses indicate that at the outset of magmatic crystallization, the mineralogical parameters display quite heterogeneous (greater symmetry) clusters (though different minerals have their discrete liquidus temperatures).
- For the lava flows, both clinopyroxene and plagioclase suggest bulk level of crystallization and terminal crystallization. The bulk level of crystallization varies from ∼30 to ∼60%, whereas termination of crystallization for the lava flows appears to be quite high (∼80 to ∼97%). The bulk level of crystallization shows a broad control of ambient temperature.
- For the dyke system [feeder dyke (FD) and chilled dyke (CD)], the bulk level of crystallization is comparable to that of lavas. However, the chilled dyke (CD) suggests early quenching, whereas the crystallization of feeder dyke (FD) was to some extent prolonged possibly because of feeding the lava flows.
- For the apparent basement rock, the cluster patterns for both clinopyroxene and plagioclase strongly suggest a relative compositional spectrum for the cumulus settled crystals, whereas the intercumulus portion corresponds to a restricted compositional range. The compositional difference between the intercumulus liquid and cumulus crystals can be ascribed to rising magma and sudden transfer below solidus.

Acknowledgements

The authors are thankful to DST-SERB (grant no. SERB/F/12254/2018-2019) for sponsoring this research project and to the authorities of IIT Bombay, India, for extending the EPMA facility. Erudite review comments from two anonymous journal reviewers are gratefully acknowledged.

Author statement

Payel Dey and Jyotisankar Ray actively participated in the field work and they prepared the geological map of the study area meticulously. Janisar M Sheikh and Suresh C Patel produced the EPMA database at IIT Bombay. Payel Dey, Jyotisankar Ray, Christian Koeberl, Suresh C Patel and Avipsha Chakraborty conceptualized the entire petrogenetic model based on hierarchical cluster analysis.

References

Ahmad M and Kumar R 2008 Petrography, composition and petrogenesis of the basalts of the Chakhla–Delakhari intrusive Complex from the eastern Deccan Volcanic Province, India; In: *Indian dykes: Geochemistry, geophysics and geochronology* (eds) Srivastava R K, Chalapathy Rao N V and Shivaji Ch, Norosa Publ. House Pvt. Ltd., pp 83–109.

Alexander P O and Paul D K 1977 Geochemistry and strontium isotopic composition of basalts from the eastern Deccan Volcanic Province, India; *Min. Mag.* **41(318)** 165–171.

Baksi A K 1994 Geochronological studies on whole-rock basalts, Deccan Traps, India: Evaluation of the timing of volcanism relative to the KT boundary; *Earth Planet. Sci. Lett.* **121(1–2)** 43–56.

Beane J E, Turner C A, Hooper P R, Subbarao K V and Walsh J N 1986 Stratigraphy, composition and form of the Deccan basalts, Western Ghats, India; *Bull. Volcanol.* **48(1)** 61–83.

Bhattacharjee S, Chatterjee N and Wampler J M 1996 Timing of the Narmada–Tapti rift reactivation and Deccan volcanism: Geochronological and geochemical evidence. Deccan Basalts; *Gond. Geol. Mag.,* Nagpur, pp. 329–340.

Bonali F L, Corazzato C and Tibaldi A 2011 Identifying rift zones on volcanoes: An example from La Réunion island, Indian Ocean; *Bull. Volcanol.* **73(3)** 347–366.

Bondre N R, Hart W K and Sheth H C 2006 Geology and geochemistry of the Sangamner mafic dike swarm, western Deccan Volcanic Province, India: Implications for regional stratigraphy; *J. Geol.* **114(2)** 155–170.

Coffin M F and Eldholm O 1994 Large igneous provinces: Crustal structure, dimensions, and external consequences; *Rev. Geophys.* **32(1)** 1–36.

Corazzato C and Tibaldi A 2006 Fracture control on type, morphology and distribution of parasitic volcanic cones: An example from Mt. Etna, Italy; *J. Volcanol. Geotherm. Res.* **158(1–2)** 177–194.

Cortes J A, Smith E I and Valentine G A 2015 Intrinsic conditions of magma genesis at the Lunar crater volcanic field (Nevada), and implications for internal plumbing and magma ascent; *Am. Mineral.* **100** 396–413.

Cox K G and Hawkesworth C J 1985 Geochemical stratigraphy of the Deccan Traps at Mahabaleshwar, Western Ghats, India, with implications for open system magmatic processes; *J. Petrol.* **26(2)** 355–377.

Crookshank H 1936 Geology of the northern slopes of the Satpuras between Morand and Sher rivers; *Geol. Surv. India Memoir* **71(2)** 173–181.

De A 1974 Short and long distance correlation of Deccan Trap lava flows; *Bull. Geol. Min. Met. Soc. India (abst)* **47** 50.

De A 1996 Entablature structure in Deccan Trap flows: Its nature and probable mode of origin; *Gond. Geol. Mag. Spec.* **2** 439–447.

Deshmukh S S, Sano T, Fujii T, Nair K K K, Yedekar D B, Umino S, Iwamori H and Aramaki S 1996 Chemical stratigraphy and geochemistry of the basalt flows from the central and eastern parts of the Deccan Volcanic Province of India; *Gond. Geol. Mag. Spec.* **2** 145–170.

Dey P, Ray J, Pandit D, Koeberl C, Ganguly S, Chakraborty S, Ghosh M and Ray I 2020 Petrogenetic aspects and role of liquid immiscibility from parts of eastern Deccan Volcanic Province, India; *Geol. J.* **55(7)** 5619–5638.

Dey P, Ray J, Sheikh J M, Patel S C and Koeberl C 2021 Windowing petrogenesis of continental flood basalts through mineralogical investigations: A case study from the Eastern Deccan Volcanic Province; *Int. J. Earth Sci.*, https://doi.org/10.1007/s00531-020-01960-3.

Duncan R A and Pyle D G 1988 Rapid eruption of the Deccan flood basalts at the Cretaceous/Tertiary boundary; *Nature* **333(6176)** 841–843.

Duraiswami R A, Bondre N R and Managave S 2008 Morphology of rubbly pahoehoe (simple) flows from the Deccan Volcanic Province: Implications for style of emplacement; *J. Volcanol. Geotherm. Res.* **177(4)** 822–836.

Eldholm O and Coffin M F 2000 Large igneous provinces and plate tectonics; *Geophys. Monogr. Am. Geophys. Union* **121** 309–326.

Ernst R E and Buchan K L (eds) 2001 Mantle plumes: Their identification through time; *Geol. Soc. Amer.* **352**.

Ganguly S, Ray J, Koeberl C, Ntaflos T and Banerjee M 2012 Mineral chemistry of lava flows from Linga area of the Eastern Deccan Volcanic Province, India; *J. Earth Syst. Sci.* **121** 91–108.

Ganguly S, Ray J, Koeberl C, Saha A, Thöni M and Balaram V 2014 Geochemistry and petrogenesis of lava flows around Linga, Chhindwara area in the Eastern Deccan Volcanic Province (EDVP), India; *J. Asian Earth Sci.* **91** 174–193.

Germa A, Connor L J, Cañon-Tapia E and Le Corvec N 2013 Tectonic and magmatic controls on the location of post-subduction monogenetic volcanoes in Baja California, Mexico, revealed through spatial analysis of eruptive vents; *Bull. Volcanol.* **75(12)** 1–14.

Hazra S, Saha P, Ray J and Podder A 2010 Simple statistical and mineralogical studies as petrogenetic indicator for Neoproterozoic Mylliem porphyritic granites of East Khasi Hills, Meghalaya, Northeastern India; *J. Geol. Soc. India* **75(5)** 760–768.

Hull P M, Bornemann A, Penman D E, Henehan M J, Norris R D, Wilson P A, Blum P, Alegret L, Batenburg S J, Bown P R and Bralower T J 2020 On impact and volcanism across the Cretaceous-Paleogene boundary; *Science* **367(6475)** 266–272.

Jennings E S, Gibson S A and Maclennan J 2019 Hot primary melts and mantle source for the Paraná-Etendeka flood basalt province: New constraints from Al-in-olivine thermometry; *Chem. Geol.* **529** 119287.

Kale V S, Dole G, Shandilya P and Pande K 2020 Stratigraphy and correlations in Deccan Volcanic Province, India: Quo vadis?; *Geol. Soc. Am. Bull.* **132(3–4)** 588–607.

Kashyap M, Shrivastava J P and Kumar R 2010 Occurrence of small scale inflated pahoehoe lava flows in the Mandla lobe of the eastern Deccan Volcanic Province; *Curr. Sci.* **98(1)** 72–76.

Korme T, Chorowicz J, Collet B and Bonavia F F 1997 Volcanic vents rooted on extension fractures and their geodynamic implications in the Ethiopian Rift; *J. Volcanol. Geotherm. Res.* **79(3–4)** 205–222.

Kumar R and Shrivastava J P 2009 Geochemistry of basic dykes from Betul-Jabalpur area in the Deccan Volcanic Province; *J. Geol. Soc. India* **74(1)** 95–107.

Le Maitre R W 1982 *Numerical petrology*; Elsevier, Amsterdam, 281p.

Lightfoot P and Hawkesworth C 1988 Origin of Deccan Trap lavas: Evidence from combined trace element and Sr-, Nd- and Pb-isotope studies; *Earth Planet. Sci. Lett.* **91(1–2)** 89–104.

Macêdo Filho A A, Archanjo C J, de Hollanda M H B M and Negri F A 2019 Mineral chemistry and crystal size distributions of mafic dikes and sills on the eastern border of the Parnaíba Basin, NE Brazil; *J. Volcanol. Geotherm. Res.* **377** 69–80.

Mahoney J, Macdougall J D, Lugmair G W, Murali A V, Das M S and Gopalan K 1982 Origin of the Deccan Trap flows at Mahabaleshwar inferred from Nd and Sr isotopic and chemical evidence; *Earth Planet. Sci. Lett.* **60(1)** 47–60.

Mahoney J J, Sheth H C, Chandrasekharam D and Pen Z X 2000 Geochemistry of flood basalts of the Toranmal section, northern Deccan Traps, India: Implications for regional Deccan stratigraphy; *J. Petrol.* **41(7)** 1099–1120.

Marzoli A, Melluso L, Morra V, Renne P R, Sgrosso I, D'antonio M, Morais L D, Morais E A A and Ricci G 1999 Geochronology and petrology of Cretaceous basaltic magmatism in the Kwanza basin (western Angola), and relationships with the Paraná-Etendeka continental flood basalt province; *J. Geodyn.* **28(4–5)** 341–356.

Mazzarini F 2004 Volcanic vent self-similar clustering and crustal thickness in the northern Main Ethiopian Rift; *Geophys. Res. Lett*, **31(4)**, https://doi.org/10.1029/2003GL018574.

Mazzarini F, Ferrari L and Isola I 2010 Self-similar clustering of cinder cones and crust thickness in the Michoacan-Guanajuato and Sierra de Chichinautzin volcanic fields, Trans-Mexican Volcanic Belt; *Tectonophys.* **486(1–4)** 55–64.

Melluso L and Sethna S F 2011 Mineral compositions in the Deccan igneous rocks of India: An overview; In: *Topics in igneous petrology* (eds) Ray J, Sen G and Ghosh B, Springer, pp. 135–159.

Moraes L C, Seer H J and Marques L S 2018 Geology, geochemistry and petrology of basalts from Parana Continental Magmatic Province in the Araguari, Uberlandia, Uberaba and Sacramento regions, Minas Gerais state Brazil; *Braz. J. Geol.* **48** 221–241.

Nair K K K, Chatterjee A K and Sano T 1996 Stratigraphy and geochemistry of the Deccan basalts along Toranmal section, western Satpura region; *Gond. Geol. Mag. Spec.* **2** 23–48.

Owen C 1989 Magmatic differentiation and alteration in isofacial green schists and blue schists, Shuksan suite, Washington: Statistical analysis of major-element variation; *J. Petrol.* **30** 739–761.

Pathak V, Patil S K and Shrivastava J P 2017 Tectonomagmatic setting of lava packages in the Mandla lobe of the eastern Deccan Volcanic Province, India: Palaeomagnetism and magnetostratigraphic evidence; *Geol. Soc. London Spec. Publ.* **445(1)** 69–94.

Pattanayak S K and Shrivastava J P 1999 Petrography and major-oxide geochemistry of basalts from the Eastern

Deccan Volcanic Province, India; *Geol. Soc. India Memoir* **2** 233–270.

Paulsen T S and Wilson T J 2010 New criteria for systematic mapping and reliability assessment of monogenetic volcanic vent alignments and elongate volcanic vents for crustal stress analyses; *Tectonophys.* **482(1–4)** 16–28.

Peng Z X, Mahoney J, Hooper P, Harris C and Beane J 1994 A role for lower continental crust in flood basalt genesis? Isotopic and incompatible element study of the lower six formations of the western Deccan Traps; *Geochim. Cosmochim. Acta* **58(1)** 267–288.

Peng Z X, Mahoney J J, Hooper P R, Macdougall J D and Krishnamurthy P 1998 Basalts of the northeastern Deccan Traps, India: Isotopic and elemental geochemistry and relation to southwestern Deccan stratigraphy; *J. Geophys. Res. Solid Earth* **103(B12)** 29,843–29,865.

Putirka K D 2008 Thermometers and barometers for volcanic systems; *Rev. Mineral. Geochem.* **69** 61–120.

Rajan S, Tiwary A and Pandey D 2005 The Deccan Volcanic Province: Thoughts about its genesis; www.mantleplumes.org/Deccan2.html.

Rao P V N, Swaroop P C and Karimulla S 2012 Mineral chemistry of Pangidi basalt flows from Andhra Pradesh; *J. Earth Syst. Sci.* **121** 525–536.

Saha A K, Bhattacharyya C and Lakshmipathy S 1974 On some problems of interpreting the correlation between the modal variables in granitic rocks; *J. Int. Assoc. Math. Geol.* **6** 245–258.

Self S, Thordarson T and Keszthelyi L 1997 Emplacement of continental flood basalt lava flows; In: *Large Igneous Provinces: Continental oceanic and planetary flood volcanism* (eds) Mahoney J and Coffin F, *Geophys. Monogr. Am. Geophys. Union,* Washington DC **100** 381–410.

Sen G and Cohen T H 1994 *Deccan intrusion, crustal extension, doming and the size of the Deccan-Reunion plume head Volcanism* (ed.) Subbarao K V, Wiley Eastern New Delhi, pp. 201–216.

Sengupta P and Ray J 2007 Mineral chemistry of basaltic lava flows from Narsingpur–Harrai–Amarwara–Lakhnadon areas of Eastern Deccan, Central India; In: *Igneous Petrology: 21st century perspective* (eds) Ray J and Bhattacharya C; Allied Publishers, New Delhi, pp. 37–72.

Sengupta P and Ray J 2011a Petrogenesis of flood basalts of the Narsingpur–Harrai–Amarwara–Lakhnadon section of Eastern Deccan Province, India; In: *Topics in Igneous Petrology* (eds) Ray J, Sen G and Ghosh B, Springer, pp. 191–238.

Sengupta P and Ray J 2011b Petrology of the mafic sill of Narshingpur-Lakhnadon section, Eastern Deccan Volcanic Province; *J. Geol. Soc. India* **77(4)** 309–327.

Sheth H C, Ray J S, Ray R, Vanderkluysen L, Mahoney J J, Kumar A, Shukla A D, Das P, Adhikari S and Jana B 2009 Geology and geochemistry of Pachmarhi dykes and sills, Satpura Gondwana Basin, central India: Problems of dyke-sill-flow correlations in the Deccan Traps; *Contrib. Mineral. Petrol.* **158(3)** 357.

Shrivastava J P, Mahoney J J and Kashyap M R 2014 Trace elemental and Nd-Sr-Pb isotopic compositional variation in 37 lava flows of the Mandla lobe and their chemical relation to the western Deccan stratigraphic succession, India; *Mineral. Petrol.* **108(6)** 801–817.

Shrivastava J P, Duncan R A and Kashyap M 2015 Post-K/PB younger ^{40}Ar–^{39}Ar ages of the Mandla lavas: Implications for the duration of the Deccan volcanism; *Lithos* **224** 214–224.

Shrivastava J P, Kumar R and Rani N 2017 Feeder and post-Deccan Trap dyke activities in the northern slope of the Satpura Mountain: Evidence from new ^{40}Ar–^{39}Ar ages; *Geosci. Front.* **8(3)** 483–492.

Snedecor G W and Cochran W G 1967 *Statistical methods*; 6th edn. Oxford and IBH Publishing Company, Calcutta, 593p.

Srinivas K N S S S, Kishore P P and Rao D S 2019 The geological site characterisation of the Mandla region, Eastern Deccan Volcanic Province, Central India; *J. Earth Syst. Sci.* **128(5)** 1–16.

Tadini A, Bonali F L, Corazzato C, Cortés J A, Tibaldi A and Valentine G A 2014 Spatial distribution and structural analysis of vents in the Lunar Crater Volcanic Field (Nevada, USA); *Bull. Volcanol.* **76(11)** 1–15.

Tibaldi A 1995 Morphology of pyroclastic cones and tectonics; *J. Geophys. Res. Solid Earth* **100(B12)** 24,521–24,535.

Valentine G A and Perry F V 2007 Tectonically controlled, time-predictable basaltic volcanism from a lithospheric mantle source (central Basin and Range Province, USA); *Earth Planet. Sci. Lett.* **261(1–2)** 201–216.

West W D 1958 The Petrography and petrogenesis of forty-eight flows of Deccan Trap penetrated by boring in Western India; *Trans Nat. Inst. Sci. India* **4** 1–56.

Yedekar D B, Aramaki S, Fujii T and Sano T 1996 Geochemical signature and stratigraphy of the Chhindwara–Jabalpur–Seoni–Mandla sector of the Eastern Deccan Volcanic Province and problems of its correlation; *Gond. Geol. Mag. Spec.* **2** 49–68.

Corresponding editor: N V Chalapathi Rao